Ocean Dynamics (2011) 61:203–215
DOI 10.1007/s10236-010-0332-0

Fine sediment transport by tidal asymmetry in the high-concentrated Ems River: indications for a regime shift in response to channel deepening

Johan C. Winterwerp

Received: 30 November 2009 / Accepted: 20 August 2010 / Published online: 9 September 2010
© Springer-Verlag 2010

Abstract This paper describes an analysis of the observed up-river transport of fine sediments in the Ems River, Germany/Netherlands, using a 1DV POINT MODEL, accounting for turbulence-induced flocculation and sediment-induced buoyancy destruction. From this analysis, it is inferred that the net up-river transport is mainly due to an asymmetry in vertical mixing, often referred to as internal tidal asymmetry. It is argued that the large stratification observed during ebb should be attributed to a profound interaction between turbulence-induced flocculation and sediment-induced buoyancy destruction, as a result of which the river became an efficient trap for fine suspended sediment. Moreover, an asymmetry in flocculation processes was found, such that during flood relative large flocs are transported at relative large flow velocity high in the water column, whereas during ebb, the larger flocs are transported at smaller velocities close to the bed—this asymmetry contributes to the large trapping mentioned above. The internal tidal asymmetry and asymmetry in flocculation processes are both driven by the pronounced asymmetry in flow velocities, with flood velocities almost twice the ebb values. It is further argued that this efficient trapping is the result of a continuous deepening of the river, and occurs when concentrations in the river become typically a few hundred mg/l; this was the case during the 1990 survey analyzed in this paper. We also speculate that a second regime shift did occur in the river when fluid mud layers become so thick that net transport rates are directly related to the asymmetry in flow velocity itself, probably still in conjunction with internal asymmetry as well. This would yield an efficient mechanism to transport large amounts of fine sediment far up-river, as currently observed.

Keywords Tidal asymmetry · Fine suspended sediment · Turbulence-induced flocculation · Sediment-induced buoyancy destruction · High concentrations · Ems River

Responsible Editor: Susana B. Vinzon

J. C. Winterwerp (✉)
Delft University of Technology, Environmental Fluid Mechanics,
P.O. Box 5048, 2600 GA Delft, The Netherlands
e-mail: j.c.winterwerp@tudelft.nl

J. C. Winterwerp
Deltares-WL|Delft Hydraulics,
P.O. Box 177, 2600 MH Delft, The Netherlands

1 Introduction

The Ems-Dollard estuary consists of the River Ems, which measures about 65 km from Hebrum weir to the river's mouth at the large tidal bay, known as the Dollard. Upstream, near Hebrum, the width of the river measures about 60 m, increasing to about 120 m near Papenbrug and around 600 m near the river mouth. The shallow and very muddy Dollard forms part of the Wadden Sea complex situated at the border between The Netherlands and Germany. The major part of the Wadden Sea and Ems-Dollard estuary seabed is fairly sandy, with exceptions, in particular in the shallow areas along the mainland. However, the seabed of the Dollard, the large tidal basin at the head of the estuary, and the Ems River are (very) muddy. The Ems River is largely situated on German territory. Figure 1 presents a schematic plan view of the Ems-Dollard estuary (after Van Leussen 1994).

Generally, the Ems's river discharge varies between around 20 and 400 m^3/s, with an average of around 100 m^3/s, and exceptional peak values as high as 1,200 m^3/s (Van Leussen 1994). During the survey discussed in the present paper, the

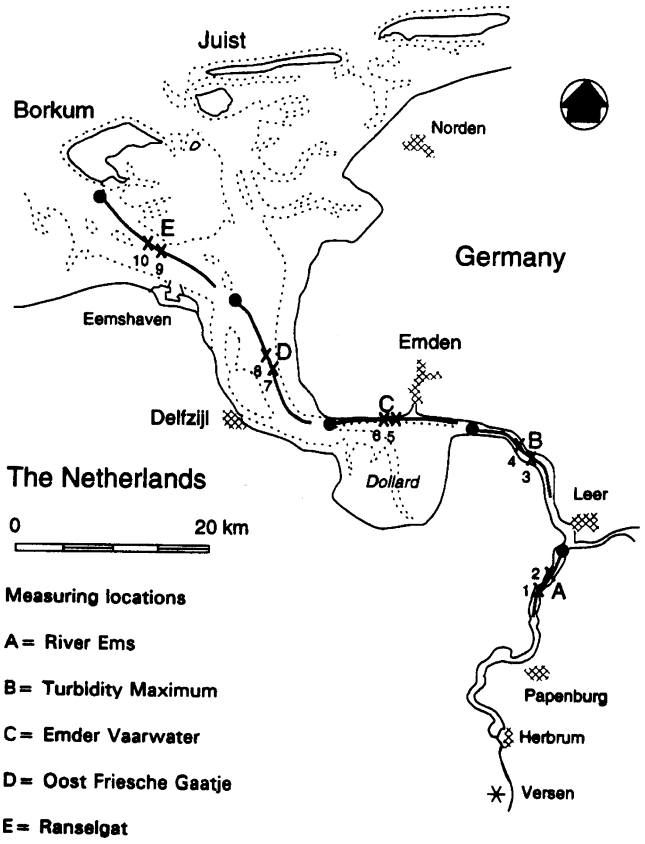

Fig. 1 The Ems-Dollard estuary—the current analysis focuses on location A (after Van Leussen 1994)

river discharge was virtually zero for a longer period of time, as a result of which salinity intrusion was about 10 km further upstream than under more average river flow conditions. The tidal range varies from around 2.5 m in the Wadden Sea (near Borkum) amplifying within the river to values over 5 m at spring tides.

The Ems-Dollard estuary in general, and the Ems River in particular have become progressively more turbid, developing from a "normal" estuary with a common estuarine turbidity maximum near the head of the salinity intrusion, to a hyper-turbid system, with mean near-surface concentrations up to 1 g/l over almost its entire length, e.g., Fig. 2. The measured time-varying concentration distribution, presented in Fig. 3 (Talke et al. 2009), reveals concentrations of fine suspended sediment over tens of grams per liter lower in the water column. Schrottke and Bartholomä (2008) presents acoustic images, showing highly dynamic fluid mud layers, measuring up to 2 m in thickness around slack water, but grossly remixed over (part of) the water column during the accelerating tide.

The large increase in turbidity levels over the last decades is attributed to an ongoing deepening of the river (e.g., de Jonge 2007). This is even more remarkable, as the sediments dredged from the river during the ongoing maintenance works are deposited well outside the river system, e.g., 15–20 km off the river mouth.

The various data described in the previous paragraphs define a highly asymmetric river system, with water depths of about 5–7 m, a tidal range varying between 3 and 5 m, and (within that depth) up to 2 m thick layers of fluid mud. Figure 4 shows that slack water occurs at high water and low water. These standing wave features are attributed to the short length of the river (~65 km), in combination with small hydraulic drag, because of the extensive occurrences of fluid mud in the river. Some reflections will be induced by the river bends upstream of Papenburg (Fig. 1). Note that the river is close to resonance, which explains the amplification of the tide along the river.

In this paper, we discuss the possible mechanisms behind the massive trapping of fines in the river. Our aim in particular is highlighting the role of the large asymmetries in the tide; and we note that this role is more complicated than in sandy systems. We hypothesize that feedback between tidal asymmetry, and the sedimentary response of the river may induce regime shifts in muddy systems towards hyper-concentrated conditions.

The literature describes many studies on the trapping of fine sediments in estuaries, forming (pronounced) turbidity maxima. Some of the results of these studies may be

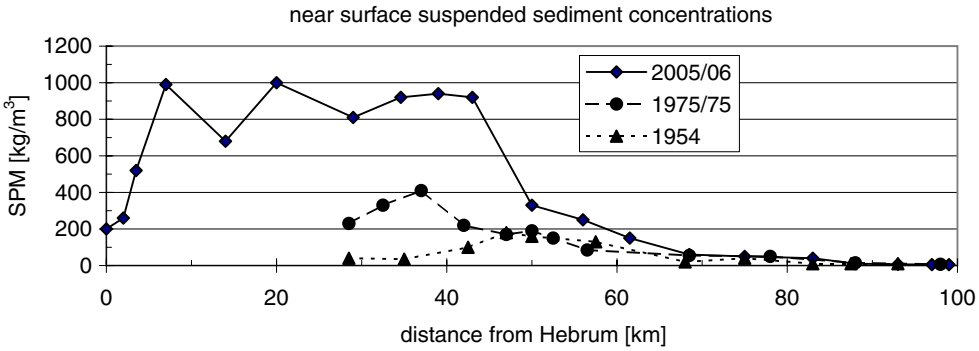

Fig. 2 Historic development of turbidity levels (SPM) in Ems-Dollard estuary (after de Jonge 2007)

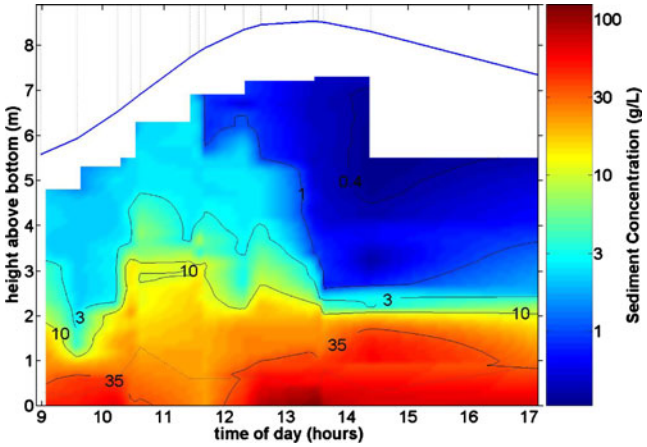

Fig. 3 Suspended sediment concentrations over time measured on Feb. 15, 2006 at km 34, Pogum in the Ems River (after Talke et al. 2009)

extrapolated explaining the large increases in turbidity in the Ems River with its deepening. These, let us say classical mechanisms, are discussed qualitatively in Section 3 of this paper. Section 4 presents an analysis of the floc size evolution over time in the river, as affected by tidal asymmetry, and Section 5 elaborates on the large flood-directed transports observed in the estuary. These analyses are supported with simulations using a 1DV POINT MODEL, the details of which are found in Section 2 and Appendix 1 to this paper. Then, in Section 6, we discuss how the various mechanisms discussed induce a regime shift from a "normal" estuarine system to the current, highly turbid river, and we speculate where similar systems could be found elsewhere in the world.

2 The 1DV POINT MODEL

The basis of the 1DV POINT MODEL is obtained by stripping all horizontal gradients from the Delft3D system (Stelling 1995) for three-dimensional simulations of hydrodynamics and the transport of matter in shallow water, except for the horizontal pressure gradient. In running the 1DV POINT MODEL, time-varying water level (depth), flow rate, and amount of matter in the water column are prescribed by the user; the 1DV POINT MODEL then establishes the vertical distribution of flow velocity and matter. The following equations, relevant for the current study, are solved in a coupled way:

- the horizontal momentum equation
- the k-ε turbulence closure model including (sediment-induced) buoyancy destruction
- the advection–diffusion equation for suspended sediment, solving the vertical mass concentration distribution of suspended sediment (more fractions are possible)
- an equation of state relating fluid density and suspended sediment concentration
- an advection–diffusion equation for the number concentration of flocs of cohesive sediment, accounting for turbulence-induced aggregation and floc breakup kinetics
- an equation relating floc size and settling velocity
- an equation for hindered settling, relating the effective settling velocity of the suspended flocs to their volume concentration
- an equation relating the mass concentration of suspended sediment with the number concentration and size of the suspended flocs
- an equation relating mass and volumetric concentration of the suspended sediment and the size of the flocs

In the current study, all sediment remains in the computational domain, i.e. there is no exchange of sediments between the water column and the sediment bed. We prescribe the measured water level and flow rate presented in Fig. 4, and an amount of fine sediment in the computational domain representing the measured depth-averaged C_0=0.61 g/l. The various coefficients of the flocculation model and the settling velocity equation have been obtained through calibration of the model against laboratory experiments by Van Leussen (1994), e.g., Winterwerp (1998).

Most equations are solved on a staggered vertical grid with an implicit numerical method. Vertical discretization is done on a sigma coordinate system, following water level

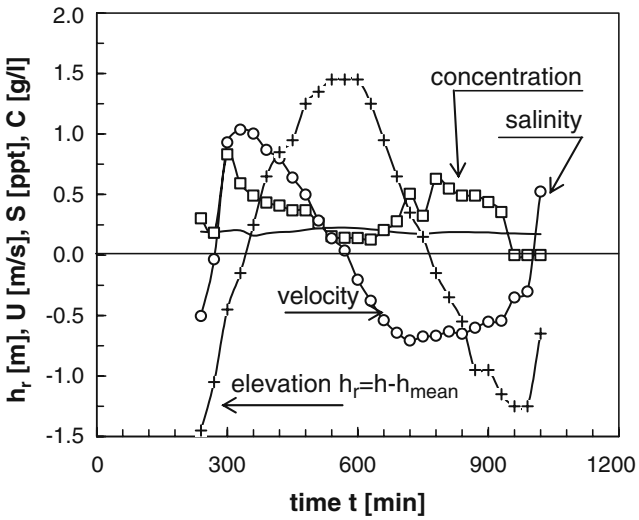

Fig. 4 Measured water level, depth-mean velocity, near-surface SPM-values and salinity at Station 2, mean tidal conditions (measurements on June 19, 1990 by Van Leussen 1994)

variations; in all simulations, 100 layers are used. The horizontal pressure gradient is obtained from a relaxation procedure by which the computed depth-averaged flow velocity equalizes the prescribed value, balancing the bed shear stress, using a quadratic friction law. The time step follows from the upwind scheme solving the advection–diffusion equation for suspended sediment. The relevant equations are summarized in Appendix 1; further details of the model are given by Winterwerp (2001, 2002).

3 Fine sediment trapping in the Ems River

In this section, we summarize a number of mechanisms responsible for the trapping of fine sediments in the Ems River and the formation of a turbidity maximum and discuss how the impact of these mechanisms is affected by a deepening of the river. We note that the majority of the fine sediments in the Ems-Dollard estuary are of marine origin, whereas riverine contributions are small, in particular since the erection of Hebrum weir. Currently, the Dollard yields a huge stock of fine sediments, which is remobilized in winter time by waves eroding the sediments from the bed (De Deckere et al. 2002) and subsequently arrested on the intertidal areas in early summer by phytoplankton activity. However, as the Dollard is accreting over longer periods of time (Cleveringa 2008), we do not expect that the Dollard yields an important net source for the fine sediments accumulating within the Ems River.

Below, we summarize the various mechanisms classically attributed to the transport and trapping of fines in estuaries and tidal rivers and the formation of an estuarine turbidity maximum (ETM) in relation to the physical properties of the sediment:

- tidal asymmetry, in particular asymmetry in the current velocity, inducing asymmetric peak velocities (e.g., Allen et al. 1980)
- internal tidal asymmetry, inducing asymmetric mixing (e.g., Jay and Musiak 1996; Scully and Friedrichs 2003)
- gravitational circulation inducing net upstream fine sediment transport towards the head of the salinity intrusion (e.g., Nichols and Poor 1967; Dyer 1997)
- lag effects (scour lag, settling lag, Postma-effect; Postma 1961)
- sediment availability in the river, such as geological deposits on/in the bed or river banks, or on/in intertidal flats, river banks, etc., supplying fines by their ongoing erosion (e.g., Dickhudt et al. 2009)
- topographical effects, such as divergence or convergence of channel cross sections (e.g., Friedrichs et al. 1998)
- asymmetry in the size, hence settling velocities of the mud flocs (e.g., Scully and Friedrichs 2007)

Note that Talke et al. (2009b) argue that also sediment-induced gravitational circulation may play a role in the Ems River, and in similar rivers elsewhere in the world. Let us investigate whether these mechanisms are relevant for the Ems River, and if so, how their impact is affected by a deepening of the river.

As mentioned in the Introduction, the Ems River is shallow, with depths of 5–7 m, and a tidal range of 3–5 m. As a result, large sub-tidal components are generated (M4 and M6), yielding a considerable asymmetry in the tide. This is depicted in Fig. 4, presenting the measured depth-averaged flow velocity at Station 2 (e.g., Fig. 1), showing flood velocities almost double the ebb velocities. As the sediment transport is a power function of the flow velocity (e.g., Section 5), the net sediment transport scales with a/h, where a is the tidal amplitude, and h is the mean water depth (e.g., Dronkers 2005)—in this case, the net transport is upstream, in the direction of the higher flood velocity. Generally, the net sediment transport induced by tidal asymmetry is explained from the nonlinear relation between the instantaneous, specific sediment transport rate T_s, and the (depth-mean) flow velocity u:

$$T_s \propto u^n \tag{1}$$

in which the exponent n is a function of the mode of transport, and typically takes values $3<n<5$ (e.g., Van Rijn 1993). Winterwerp (2001) (see also Winterwerp and Van Kesteren 2004) showed that also for cohesive sediment a sediment transport formula can be derived if fines are abundant. For capacity conditions, i.e. in case of unlimited availability of fine sediment, a saturation concentration C_s can be defined which depicts the maximum load of fine sediment which can be kept in suspension by the turbulent flow. When this load is exceeded, the turbulent field collapses, and fluid mud is formed.

For cohesive sediment under capacity conditions, the transport rate follows from $u \times C_s$ (e.g., Winterwerp 2001):

$$T_s \propto u^4/hw_s \tag{2}$$

where h is the water depth, and w_s the (effective) settling velocity of the mud flocs. Hence, we expect a strong effect of tidal asymmetry on the net sediment transport in the Ems River. But, due to deeper water and lower flow velocities, a deepening of the river would yield a decrease in the net upstream fine sediment transport. However, the asymmetry is still pronounced, and the Ems River remains profoundly flood dominant, though the transport rate, according to classical theory, may have decreased over time. In Section 6,

we discuss how the role of tidal asymmetry has changed over time and has influenced the evolution of the sedimentary features of the Ems River.

Jay and Musiak (1996) analyzed the effects by an asymmetry in vertical mixing induced by differences in the magnitude of ebb and flood velocities—this mechanism is referred to as internal tidal asymmetry. Generally, internal asymmetry affects net sediment transport in estuaries through its effect on the (vertical) salinity distribution, e.g., through a difference in vertical stratification during ebb and flood. Yet, also differences in the vertical distribution of the suspended fine sediment may result in net transports when larger concentrations are found in the upper part of the water column, where velocities are higher. Asymmetry in vertical mixing indeed plays a major role in the Ems River, as elaborated in Sections 4 and 5, and as such, it can be argued that internal tidal asymmetry plays an important role in the sediment dynamics in the river. As asymmetry in vertical mixing is induced by asymmetry in flow velocity, we expect that the effect of internal tidal asymmetry will scale with a/h, as well, implying a less pronounced effect with the deepening of the river. Yet, we will see in Sections 4 and 5 that the effects of asymmetrical mixing have become very large in the Ems River. Note that in response to the river's deepening, two opposing mechanisms play a role: deepening would decrease the phase difference between the higher harmonics, but the amplitude of the components increases. In general, though, the effect of tidal asymmetry decreases when the river depth increases.

Net sediment transport by gravitational circulation is the result of a change in the vertical velocity profile induced by horizontal salinity gradients, in conjunction with a vertically non-homogeneous suspended sediment concentration distribution (e.g., Dyer 1997). For a vertical homogeneous salinity distribution, the induced residual flow velocity scales with h^2/u_* (e.g., Winterwerp et al. 2006) and would, therefore, rapidly increase with river depth. With increasing vertical stratification, the effects of gravitational circulation increase—vertical stratification itself increases with depth (e.g., Eq. 3, Pritchard 1952).

Pritchard (1952) introduced the estuary number E_D, a kind of inverse flux Richardson number, classifying estuaries with respect to vertical mixing:

$$E_D = \frac{P_t}{Q_f T} \frac{u_{\max}^2}{gh\Delta\rho/\rho} \tag{3}$$

where Q_f is the river flow discharge, T is the tidal period, P_t is the tidal prism, $u_{\max}$, and h are the maximum flow velocity and water depth in the mouth of the estuary, and $\Delta\rho/\rho$ is the horizontal salinity-induced density gradient. When $E_D<0.25$, an estuary is expected to be vertically stratified, whereas well-mixed conditions are expected for $E_D>10$.

Large gradients in vertical suspended sediment concentration will have a profound effect on the vertical mixing rates in the estuary. This may lead to sediment-induced stratified salinity distributions, even when Pritchard's E_D would predict otherwise. This is demonstrated in Fig. 5, showing two typical profiles of the tidally averaged salinity distribution in the Suriname River (Loose 2008). These profiles are fairly stratified, though $E_D\approx15$. As an increase in salinity distribution enhances the effects of gravitational circulation, the interaction between the vertical distribution of suspended sediment and salinity, and vertical mixing yields a pronounced positive feedback mechanism: the augmented vertical salinity stratification induces an increase in the import of fine sediment by gravitational circulation, which augments the vertical salinity stratification further, etc.

We did not find data indicating similar salinity stratification in the Ems River, which may be due to the very low fresh water flow in the river; for typical conditions in the Ems River, $E_D\approx100$.[1] Most likely, this feedback therefore does not play a role in the Ems River.

Postma (1961) recognized that a decrease in flow velocity towards the head of an estuary, in conjunction with an erosion (resuspension) threshold of fine sediment, would result in net upstream transport of fine sediment – this mechanism is generally referred to as the settling lag. More general, the turbulent energy to keep sediment in suspension is smaller than required for resuspension. As a result, asymmetries in the duration of the high and low water slack periods induce a net transport of fine sediments, as elaborated by Dronkers (2005). Though theoretically these classical lag-effects may play a role in the Ems River, we believe they are well-overshadowed by the lag effects induced by tidal asymmetry (Section 5) and flocculation (Section 4).

In some estuaries, an uneven availability of fine sediment in the riverbed may result in local increases in turbidity, such as the formation of an ETM. Also, large intertidal areas and a network of channels, c.q. ebb and flood channels may induce a considerable net transport of fine sediment in one direction. As the Ems River consists of a fairly one-dimensional channel, with few intertidal banks, we do not expect that these effects are too important for the net transport of fines in the river.

Previous work by Winterwerp (2002) demonstrated the importance of flocculation and sediment-induced buoyancy

[1] Note that the June 1990 measurements elaborated in the next sections have been carried out upstream of the salinity intrusion, and the analysis in this paragraph is not relevant for these June data.

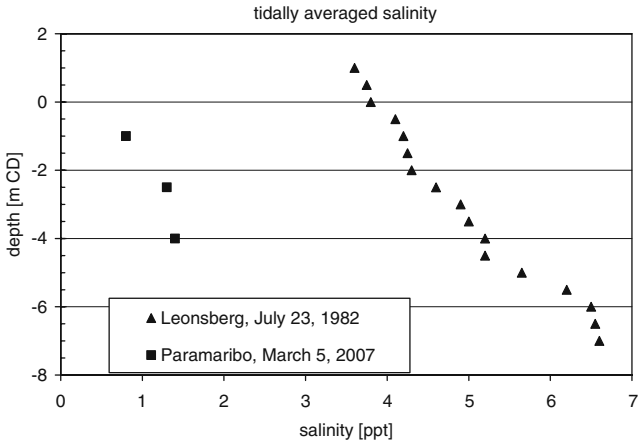

Fig. 5 Measured tidally averaged salinity distributions in the Suriname River (Loose 2008)

destruction on sediment dynamics in systems with higher suspended sediment concentrations. This effect will therefore be analyzed in more detail in Section 4. The effect of tidal asymmetry in floc size, maximum flow velocity, and vertical mixing on net transport into the Ems is evaluated in Sections 5 and 6.

4 Asymmetry in floc formation

The Station 2 measurements by Van Leussen (1994) are presented in the form of isolutals[2] in Fig. 6, showing two pronounced features, i.e. a fairly well-mixed suspended sediment concentration distribution during flood, rapid settling around high water slack (HWS) and pronounced stratification during ebb. Winterwerp (2002) presents an analysis of these data using the 1DV-model described in Section 2. He concluded that this rapid settling and stratification can only be reproduced/explained properly if the effects of flocculation and buoyancy destruction are both accounted for in the model. In Fig. 7 the results of these 1DV simulations are shown; further details and a more elaborate comparison with the data are given in Winterwerp (2002).

The rapid settling during HWS is attributed to rapid floc formation, which can be understood from the relation between the (equilibrium) floc size and ambient parameters, e.g., large suspended sediment concentration and low turbulence levels:

$$D_e = D_p + \frac{k_A c}{k_B \sqrt{G}} \text{ with } G = \sqrt{\frac{\varepsilon}{\nu}} = \frac{\nu}{\lambda_K^2} \tag{4}$$

where D_e is the equilibrium floc size, D_p is the size of the primary particles (floc building entities), c is the suspended sediment concentration by mass, G is the turbulent shear rate at the Kolmogorov scale λ_K, ν is the fluid's kinematic viscosity, ε is the dissipation rate per unit mass of the turbulent flow, and k_A and k_B are flocculation and floc breakup coefficients, respectively (for details, see Winterwerp 1998). Equation 4 predicts larger flocs higher in the water column where turbulence levels are lower than near the bed, as commonly observed. As suspended sediment concentrations are high, the flocculation time T_f is small, and large flocs can indeed be formed around slack water (e.g., Winterwerp 1998):

$$\text{for} \quad D_e >> D_0 \quad T_f \approx (k_A c G D_0)^{-1} \tag{5}$$

where D_0 is the initial floc size.

The large stratification during ebb is attributed to a strong interaction between flocculation and buoyancy destruction. This is illustrated in Fig. 8a, showing relatively large settling velocities lower in the water column during ebb, computed with the 1DV-model. This yields a highly stable concentration profile, with pronounced damping of vertical mixing, as illustrated by the eddy viscosity profiles in Fig. 9. In this case, the more common situation is reversed, and we find the larger flocs lower in the water column. Figure 8a shows that this reversal starts around HWS and prevails to the next flood period (results not shown). For comparison, the time variations in floc size measured by Van Leussen (1994) are presented in Fig. 8b, showing comparable values and a similar asymmetry in size over ebb and flood.

Sustaining these arguments further, vertical profiles of eddy viscosity are also computed with the 1DV-model in which either the effects of flocculation or of buoyancy destruction are switched off. Figure 9 shows that the strong damping of vertical mixing, hence, the strong stratification during ebb is only found when the full 1DV-model is used. Winterwerp (2002) presents further results and discussions in the form of isolutals throughout the tide, and shows how computed floc sizes agree with observations.

In terms of Eq. 4, one may summarize the computational observations as follows: during flood, the effects of turbulence (G) govern the vertical floc size distribution, whereas the suspended sediment concentration (c) is only responsible for the actual size of the flocs. This is the more common situation in rivers, estuaries and coastal seas. However, during ebb, the vertical floc size distribution is dominated by the effects of the suspended sediment concentration; the effects of gradients in turbulence are small, as turbulence is largely damped. This picture can be attributed directly to the large asymmetry in tidal flow

[2] Isolutals are lines of equal concentration in suspended sediment.

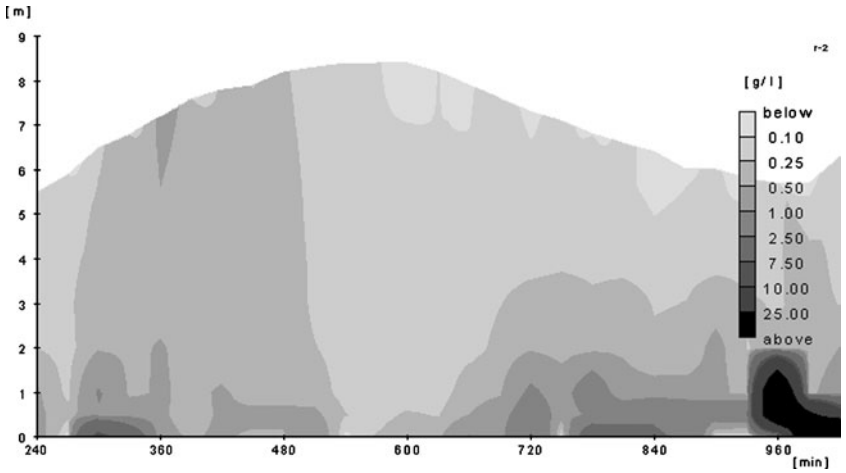

Fig. 6 Measured isolutals at Station 2, June 19, 1990. Note rapid settling just prior to high water and pronounced stratification during ebb (after Van Leussen 1994)

velocity, with the much larger velocities during flood, as explained above: the kinetic energy for vertical mixing during flood is much larger than during ebb—see also Section 5. Yet, this behavior during ebb can only become manifest if the suspended sediment concentrations are large enough. If not, buoyancy destruction would be too small to induce the predicted stratification patterns.

The asymmetry in floc size formation over the tidal period has an important consequence for the transport of flocs of different size. The observations above are summarized in the cartoon of Fig. 10. During flood, large flocs high in the water column are transported into the estuary at relatively large flow velocity (not only because of the asymmetry in flow velocity, but also because flow velocities higher in the water column are larger than near the bed). During ebb, on the contrary, the larger flocs are expected near the bed, transported out of the estuary at much smaller flow velocities. This must have a large effect on the trapping efficiency in the estuary: from HWS to the next flood, the river's trapping efficiency apparently is very high, e.g., Section 5.

The asymmetry in floc size distribution is further illustrated in Fig. 11, showing the computed and observed variation of the "floc transport rate" over the tidal period. The computed floc transport rate T_f is defined as:

$$T_{f,model} = \int_h u(z) D_f(z) dz \tag{6}$$

As sufficient details in floc size distribution were not given by Van Leussen (1994), we define the measured floc transport rate differently:

$$T_{f,data} = U W_s h \tag{7}$$

The vertical axes in Fig. 11 are scaled allowing a direct comparison of the measured and computed floc transport rate, showing that both variations depict a very similar behavior. Integration over the flood and ebb period, respectively, shows a net flood-dominated "transport of floc size" ~20% larger than the transport during ebb, according to both the measurements and the 1DV-computations. Note that this diagram does not yield information on the net mass transport—it only tells us that

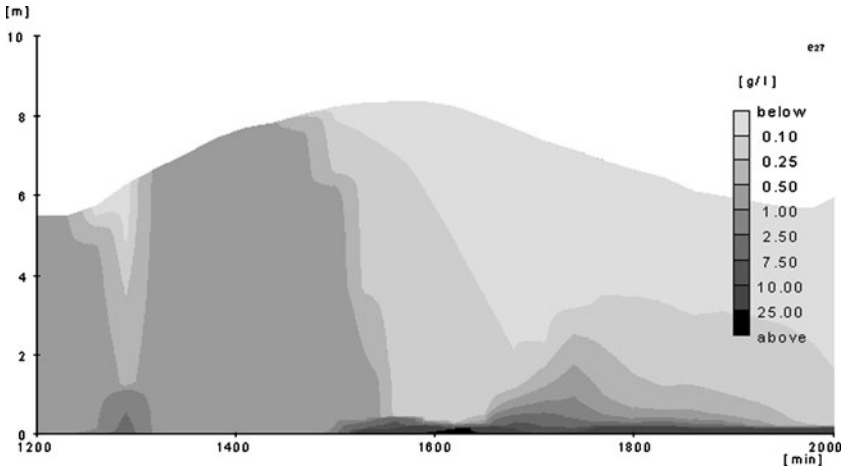

Fig. 7 Computed isolutals at Station 2, June 19, 1990. Note rapid settling just prior to high water and pronounced stratification during ebb

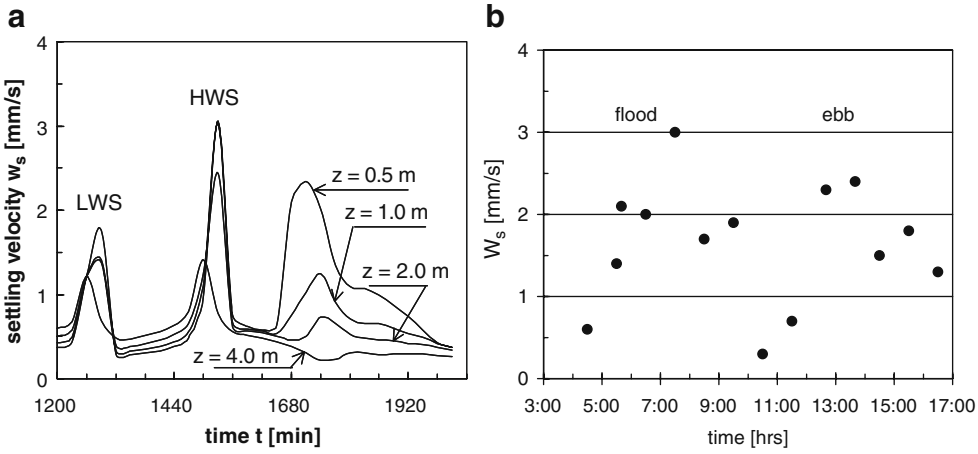

Fig. 8 **a** Computed variation in settling velocity; during slack water, large settling velocities are predicted. During flood, the larger settling velocities are found higher in the water column, whereas during ebb, a stable settling velocity distribution develops with the larger settling velocity near the bed (after Winterwerp 2002); bed at z=0. **b** Measured floc size variation over tidal cycle (redrawn after Van Leussen 1994). These measurements were done with a video camera mounted to a settling tube, floating 1.5 m below the water surface

larger flocs are transported into the estuary during flood, whereas smaller flocs leave the estuary during ebb.

5 Net fine sediment transport

Let us analyze the transport rates at Station 2 (Fig. 1), further to our analysis in Section 4. Van Leussen established the fine sediment transport rate at his five measuring locations and found flood dominance in all cases. Figure 12 presents his analysis for Station 2, showing a specific (i.e. per unit width) net flood-directed transport of 8.5 kg/m upon integration over the tide. The transport rate computed with the 1DV POINT MODEL is also presented in Fig. 12, comparing reasonably with Van Leussen's data, yielding a net flood-directed fine sediment transport, integrated over the tidal period, of 10.4 kg/m, i.e. about 15% larger than measured. We note that the maximum value of the fine sediment transport during flood is only about twice the maximum value predicted (and measured) during ebb and not the factor of around 16, suggested by Eq. 2 for a flood velocity twice the ebb velocity. We believe this is due to the non-capacity conditions during flood. In the 1DV POINT MODEL, the initial, vertically homogeneous sediment concentration was set at 0.6 g/l, after some trial and error but consistent with the observations. For larger concentrations in the water column, the computed turbulence field collapsed during ebbing conditions, when peak flow velocities were considerably smaller than during flood. We anticipate that also in the Ems River itself during the evolution phase of the river at the time of the 1990 surveys, the sediment load that is mobile throughout a tidal cycle was largely governed by the ebb conditions. This would explain the still fairly modest response of net sediment transport to the large asymmetry in tidal velocity (see also Section 6).

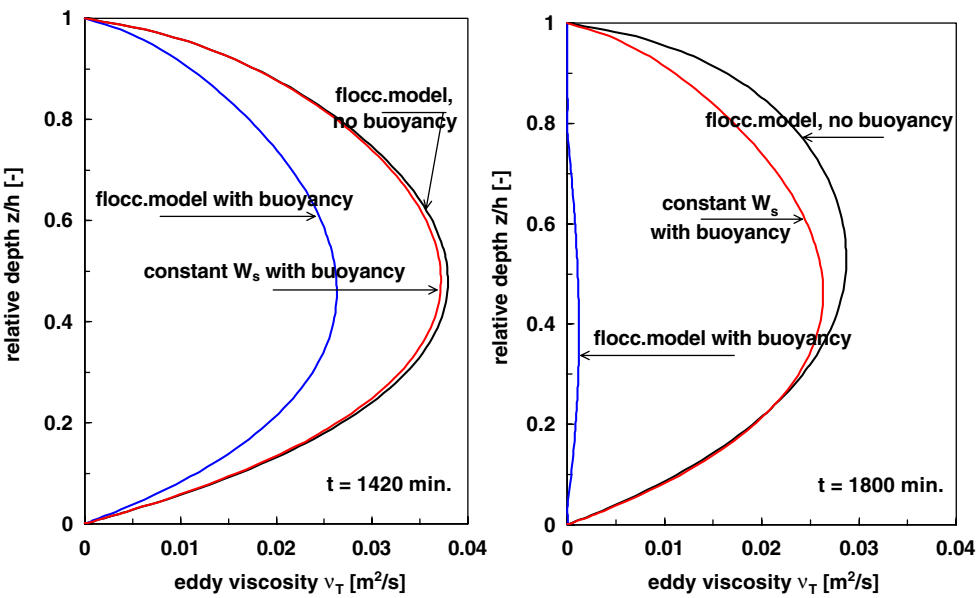

Fig. 9 Computed eddy viscosity profiles during flood (*left panel*) and during ebb (*right panel*). Note the collapse of vertical mixing predicted with the full 1DV model (flocculation and buoyancy destruction) explaining strong stratification during ebb

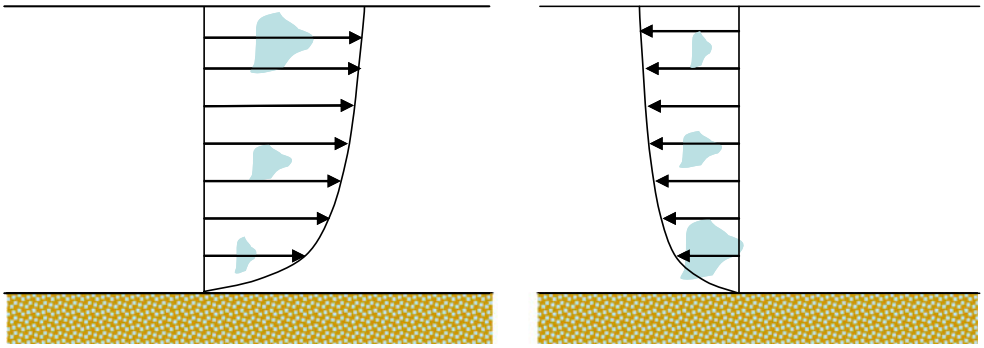

Fig. 10 Cartoon of mud flocs transported during flood (*left panel*) and during ebb (*right panel*)

Winterwerp (2002) ran the 1DV POINT MODEL as well for two other model configurations, i.e. with a constant settling velocity (but with sediment-induced buoyancy destruction) and without sediment-induced buoyancy destruction (but with the full flocculation model). The computed fine sediment transport rates are presented in Fig. 12, showing that for these cases, the simulations predict a specific net ebb-directed transport of −2.7 and −4.1 kg/m. The computed transport during flood seems to be fairly insensitive to the model settings, though the full model predicts somewhat smaller rates around slack water, which can be attributed to the rapid settling prior to high water. On the contrary, the computed results are very sensitive to the model configuration during ebb: the ebb-directed transport computed with the full model is much smaller than computed with the two other configurations. Figures 6 and 7 suggest that the differences in sediment transport are mainly due to the large stratification during ebb, which can only be captured reasonably with the full 1DV POINT MODEL. This large trapping is enhanced by the asymmetry in flocculation described in Section 4, which is explicitly accounted for in the full 1DV POINT MODEL.

6 Discussion and conclusions

In this paper, we have presented a further analysis of the substantial flood-dominated transport of fine sediment measured in the Ems River by Van Leussen (1994) in June 1990. Though the river flow in that survey period, and in the previous weeks, was very low, we believe that the conditions are characteristic for the river in that era of its evolution. In our analysis, we may apply a 1DV POINT MODEL, because the horizontal gradients in hydro-sedimentological parameters were small (Winterwerp 2002).

At Station 2, subject of the current analysis, the measured suspended sediment pattern is characterized by a rapid settling around HWS and profound stratification during ebb. These features could be reproduced qualitatively with the 1DV POINT MODEL, provided that turbulence-induced flocculation and sediment-induced buoyancy destruction are accounted for. From a sensitivity analysis with the model, we infer that the rapid settling around HWS should be attributed to rapid flocculation of the suspended sediment when flow velocities decrease towards the end of the flood, whereas stratification

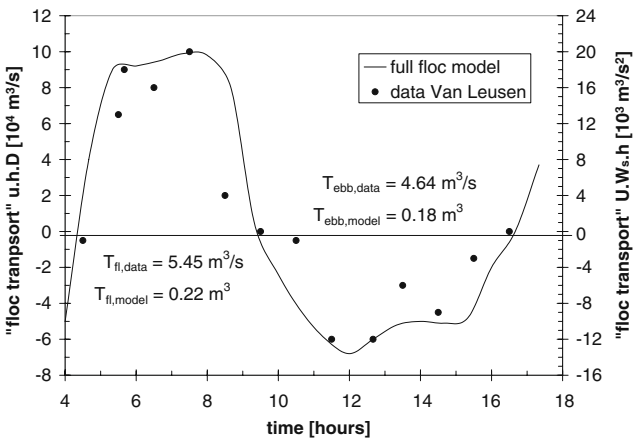

Fig. 11 Measured and computed "floc transport rate"—see text for explanation

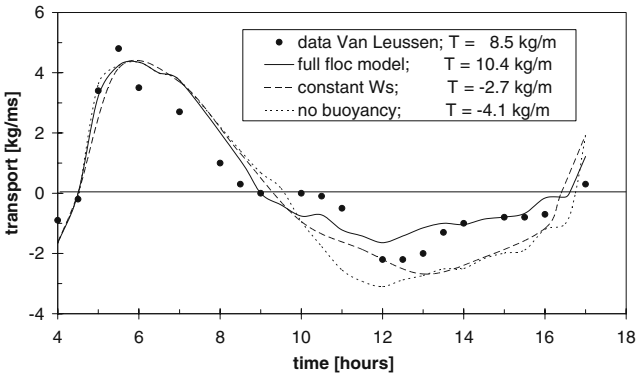

Fig. 12 Measured and computed sediment transport rate at Station 2; computations with the full 1DV model with full flocculation and buoyancy destruction, with the full 1DV model, but constant settling velocity and with the full 1DV model, but without buoyancy destruction

during ebb is the result of a strong interaction between flocculation processes and sediment-induced buoyancy destruction. This analysis also suggests that during flood relatively large flocs are transported up-river, whereas during ebb, smaller flocs are transported down-river. This picture is qualitatively similar to Van Leussen's (2009) observations, who concluded that floc size decreases up-estuary, though he attributes this to biochemical effects on the flocculation process.

The 1DV POINT MODEL also predicts a flood-oriented transport of fine sediments of the same order of magnitude as Van Leussen's observations, again provided that turbulence-induced flocculation and sediment-induced buoyancy destruction are accounted for. If not, the model predicts export of fine sediment. This change in model behavior is almost entirely due to the effects of the stratification during ebb; fine sediment transport during the flood is hardly affected by the model configuration. In other words, the large net up-river fine sediment transport is caused by large trapping of fines during ebb, owing to strong sediment-induced stratification and relatively large floc sizes near the bed.

It is remarkable that the computed (peaks in) flood and ebb transport do not reflect the large asymmetry in transport capacity given by Eq. 2, which would imply an order of magnitude difference between flood and ebb transport. This anomaly seems to be caused by the limited amount of fines available for transport during flood—this amount seems to be determined by ebb conditions. A measure for the capacity conditions (during ebb) is given by the saturation concentration C_s in the river:

$$C_s \approx 0.023U^3/hW_s, \tag{8}$$

amounting to about 500 mg/l for U=0.5 m/s, h=5, and W_s= 1 mm/s for ebb conditions (Winterwerp and Van Kesteren 2004). This value is well in the range of the depth-mean concentration found by Van Leussen (1994) and which had to be prescribed in the 1DV POINT MODEL to represent the 1990 observations by Van Leussen (1994).

We have argued that the trapping effects of gravitational circulation must have increased with ongoing deepening of the river. However, given the large effects of tidal asymmetry, we presume that these effects are relatively small. This presumption is further substantiated by the observation of Fig. 2 that currently, the river no longer depicts a profound turbidity maximum near the head of the salinity intrusion, but the river has become turbid over its entire length.

From these observations, we may deduce how the river responded to ongoing deepening. We have no data on the transition of the Ems River from a "normal" turbid river into its current, hyper-concentrated state over the time period shown in Fig. 2. Therefore, we have developed a conceptual picture for the transition of the river as a result of deepening from its former equilibrium, using our observations described on the previous pages. This picture is summarized in Table 1. We start a long time ago from a long-term equilibrium, referred to as phase 0 in Table 1, at which up-river directed fine sediment transport induced by gravitational circulation and the various effects of tidal asymmetry balance the down-river transport induced by the river flow. The fine sediments in the Ems River are mainly marine-born, though some sediment may be delivered by the river. Over shorter time periods, accumulation or flushing may occur, as a result of e.g., varying river flows. Under these conditions, the formation of an ETM is expected near the head of the saline intrusion. Over longer time scales, land formation initiated on vegetated mudflats may reduce the river's tidal volume, affecting the long-term morphodynamic equilibrium.

As a response to deepening, net accumulation is expected, restoring equilibrium, Phase 1, Table 1. The underlying processes are a decrease in river-induced flushing, as river flow velocities decrease in proportion to the river's cross section, in conjunction with an augmented net transport by gravitational circulation, as water depth increase. Deepening would also reduce the generation of overtides, but the tidal amplitude itself increases. It is, therefore, not possible to predict the net effect of deepening on tidal asymmetry without detailed hydrodynamic modeling, though a decrease in asymmetry is expected in general. Possibly, reduced vertical mixing already starts to play a role, enhancing the trapping efficiency of the river (see below). As the accumulating fine sediments do not form a rigid bed immediately, also turbidity levels increase, as more sediments are available for remobilization, and suspended sediment concentrations in the ETM increase.

A further increase of the river's depth would increase the amount of remobilizable sediments further, accompanied by a further increase in suspended sediment concentrations. When the riverbed becomes predominantly muddy, as the Station 2 conditions analyzed in the current study, profound feedbacks between the various processes are expected through which the river evolves into its present hyper-concentrated state. In this regime, gravitational circulation still plays a role, but its effect is small compared to the dominant contributions of internal tidal asymmetry, with profound differences in vertical mixing during ebb and flood: during ebb, the river is highly stratified by sediment-induced buoyancy destruction. ETM suspended sediment concentrations become high, and also beyond this ETM elevated suspended sediment concentrations are expected, possibly owing to sediment-induced gravitational circulation as well (Talke et al. 2009b).

Table 1 Summary of Ems River response to its deepening

Phase	Dominant transport processes		Comments
	Flood-directed transport	Ebb-directed transport	
0	"Normal" estuary with ETM; equilibrium[a]		Long-term balance between ebb and flood transport
	(Slack water) tidal asymmetry; Gravitational circulation	River-induced flushing	
1	Small disturbance; transient state		Net import
	(Slack water) tidal asymmetry? Enhanced gravitational circ	Reduced river-induced flushing	Weak feedback
2	Large disturbance; transient state		large Net import
	Internal tidal asymmetry: mixing and floc size		Strong feedback
	Limited sediment load and determined by ebb conditions		Large trapping
	Fairly well-mixed flood	Stratified ebb	
	Relative unimportant grav. circ.;	Fluid mud	
	Sediment-induced grav. circ. ?	Small ebb transport	
3	Hyper-concentrated estuary; new equilibrium[b]		Large net import
	Asymmetry in tidal velocity		Strong feedback
	Internal tidal asymmetry Pronounced fluid mud formation		Large trapping
	Capacity conditions; transport formula applicable		

See text for further explanation; river depth in Phases 2 and 3 are not necessarily larger than in Phase 1

Phase 0 "undisturbed" state of the river

[a] Long-term equilibrium may be disturbed by land formation, reducing estuary's tidal volume

[b] Without maintenance, estuary may return towards its original state if a rigid bed can be formed

Our analysis with the 1DV POINT MODEL suggests that this regime shift becomes imminent in the Ems River at concentrations typically of the order of a few 100 mg/l. Then, the trapping efficiency of the river increases rapidly as a result of vertical stratification during ebb, and asymmetry in floc size. The rate at which the river really accumulates fine sediments is determined merely by the supply of these sediments from the Wadden Sea–Dollard estuary, than by internal hydro-sedimentological processes.

We anticipate a second regime shift in the estuary, Phase 3, Table 1, when the river starts to develop pronounced occurrences of fluid mud, as observed presently by Schrottke and Bartholomä (2008). In that case, fine sediment transport rates are expected to be dominated by the tidal asymmetry of the peak currents themselves, as described with Eq. 7. Now re-entrainment of the fluid mud layers, which scales with U^3 as well, becomes a dominant mechanism. Sediment is transported up-river towards the river's head at Herbun by the large tidal asymmetry, and the entire river becomes highly turbid. As the consolidation rate of fluid mud layers scales with their thickness squared, we expect that the properties of the fluid mud layer are fully determined by the velocities during flood conditions. Note that not much consolidation of the thick fluid mud layers during ebb is expected.

In summary, we infer that in response to deepening of the Ems River, the sediment load in the river first increases through an increase in the up-river transport by gravitational circulation and a decrease in river-induced flushing. Then, in the second phase of the river's transition towards its hyper-concentrated state, when the concentration in the river attains values of a few 100 mg/l, internal tidal asymmetry becomes dominant because of pronounced interactions between the sediment load, and the turbulent water movement and vertical mixing. We believe that the 1990 survey conditions fall within this second phase of development. Finally, the load of fine sediment becomes so large that in the final phase of the river's evolution, thick fluid mud layers are formed, and the up-river fine sediment transport is dominated by tidal asymmetry of the current velocity. The second phase in transition is probably not stable: trapping is so large that a further development towards the final phase may be inevitable; the time scale of this intermediate phase depends mainly on the sediment supply and may amount to a decade or so, as in the Ems River.

We presume that the regime shifts described above have also occurred in other highly-turbid shallow rivers, which are characterized by a profound tidal asymmetry. Hence, such rivers are likely to be encountered in meso- and macro-tidal environments. One example is the Loire River: even the very large river flows occurring at times in this river do not reverse the effects of tidal asymmetry, and cannot flush the fine sediments completely. The river remains highly turbid throughout the year, though the location of the estuaries turbidity maximum may vary with time (Le Hir 1997).

Acknowledgements I would like to acknowledge my colleague Dr. Bas Van Maren for his valuable comments on an earlier draft of the manuscript. I also like to thank Dr. Stefan Talke for making available Fig. 3.

Appendix 1—The 1DV POINT MODEL

The 1DV equation for horizontal momentum reads:

$$\frac{\partial u}{\partial t}+\frac{1}{\rho}\frac{\partial p}{\partial x}=\frac{\partial}{\partial z}\left[(\nu+\nu_T)\frac{\partial u}{\partial z}\right] \tag{9}$$

The pressure term in (9) is adjusted to maintain a given, time-dependent depth-averaged velocity:

$$\frac{1}{\rho}\frac{\partial p}{\partial x}=-\frac{\tau_\mathrm{b}}{\rho h}+\frac{U(t)-U_0(t)}{T_\mathrm{rel}},\quad U(t)=\frac{1}{h}\int_{z_\mathrm{bc}}^{Z_\mathrm{s}}u(z',t)\mathrm{d}z' \tag{10}$$

The standard k–ε model, i.e. with the common coefficients with sediment-induced buoyancy destruction reads:

$$\frac{\partial k}{\partial t}=\frac{\partial}{\partial z}\left\{(\nu+\nu_T)\frac{\partial k}{\partial z}\right\}+\nu_T\left(\frac{\partial u}{\partial z}\right)^2+\frac{g}{\rho}\Gamma_T\frac{\partial \rho}{\partial z}-\varepsilon \tag{11}$$

$$\frac{\partial \varepsilon}{\partial t}=\frac{\partial}{\partial z}\left\{\left(\nu+\frac{\nu_T}{\sigma_\varepsilon}\right)\frac{\partial \varepsilon}{\partial z}\right\}+c_{1\varepsilon}\frac{\varepsilon}{k}\nu_T\left(\frac{\partial u}{\partial z}\right)^2 +(1-c_{3\varepsilon})\frac{g}{\rho}\Gamma_T\frac{\varepsilon}{k}\frac{\partial \rho}{\partial z}-c_{2\varepsilon}\frac{\varepsilon^2}{k} \tag{12}$$

The advection–diffusion equation for the mass concentration of suspended sediment reads:

$$\frac{\partial c^{(i)}}{\partial t}-\frac{\partial}{\partial z}\left\{w_\mathrm{s}^{(i)}c^{(i)}\right\}-\frac{\partial}{\partial z}\left\{\left(D_\mathrm{s}^{(i)}+\Gamma_T^{(i)}\right)\frac{\partial c^{(i)}}{\partial z}\right\}=0 \tag{13}$$

Water density and suspended sediment concentration are related through the equation of state:

$$\rho\left(c^{(i)}\right)=\rho_\mathrm{w}+\sum_{(i)}\left\{\left(1-\frac{\rho_\mathrm{w}}{\rho_\mathrm{s}^{(i)}}\right)c^{(i)}\right\} \tag{14}$$

The advection–diffusion equation for the number concentration of suspended flocs accounts for turbulence-induced flocculation through an aggregation term (1st term in RHS (15)) and a floc breakup term (2nd term in RHS (15)).

$$\frac{\partial N}{\partial t}+\frac{\partial}{\partial z}\left(\frac{(1-\phi_*)(1-\phi_\mathrm{p})}{(1+2.5\phi_\mathrm{f})}w_{\mathrm{s,r}}N\right)-\frac{\partial}{\partial z}\left(\Gamma_t\frac{\partial N}{\partial z}\right)= -k_\mathrm{A}'k_N^3(1-\phi_*)Gc^{\frac{3}{n_f}}N^{\frac{2n_f-3}{n_f}} +k_\mathrm{B}'k_N^{2q}G^{q+1}\left(k_Nc^{\frac{1}{n_f}}N^{\frac{-1}{n_f}}-D_\mathrm{p}\right)^p c^{\frac{2q}{n_f}}N^{\frac{n_f-2q}{n_f}} \tag{15}$$

The settling velocity of single flocs in still water and its effective value by hindered settling are given by:

$$w_{\mathrm{s,r}}=\frac{\alpha}{18\beta}\frac{(\rho_\mathrm{s}-\rho_\mathrm{w})g}{\mu}D_\mathrm{p}^{3-n_f}\frac{D_\mathrm{f}^{n_f-1}}{1+0.15Re_\mathrm{f}^{0.687}} \tag{16}$$

$$w_{\mathrm{s,eff}}=\frac{(1-\phi_f)^2(1-\phi_\mathrm{s})}{1+2.5\phi_f}w_{\mathrm{s,r}} \tag{17}$$

These equations are completed by geometrical relations between number concentration, mass concentration, volumetric concentration and floc size:

$$N=\frac{1}{f_\mathrm{s}}\frac{c}{\rho_\mathrm{s}}D_\mathrm{p}^{n_f-3}D_\mathrm{f}^{-n_f} \tag{18}$$

$$\phi_\mathrm{f}=\left(\frac{\rho_\mathrm{s}-\rho_\mathrm{w}}{\rho_\mathrm{f}-\rho_\mathrm{w}}\right)\frac{c}{\rho_\mathrm{s}}=\frac{c}{\rho_\mathrm{s}}\left[\frac{D_\mathrm{f}}{D_\mathrm{p}}\right]^{3-n_f} \tag{19}$$

This system of equations is closed with a set of boundary conditions, which, however, are not presented in this paper; the reader is referred to Winterwerp (2002). In these equations, the following symbols are used:

- $c^{(i)}$ sediment concentration by mass for fraction (i)
- D_f diameter of mud flocs
- D_p diameter of primary particles
- D_s molecular diffusion coefficient for sediment
- G shear rate parameter; $G=\sqrt{(\varepsilon/\nu)}$
- k turbulent kinetic energy
- k_A flocculation parameter
- k_B floc breakup parameter

N number concentration of the mud flocs
n_f fractal dimension
p pressure
q empirical coefficient; q=0.5
t time
T_{rel} relaxation time
U actual computed depth-averaged flow velocity
U_0 prescribed depth-averaged flow velocity
u horizontal flow velocity, positive in x-direction
z_{bc} apparent roughness height
w_s effective settling velocity
$w_{s,r}$ settling velocity of individual particle
x horizontal coordinate
z vertical coordinate
Γ_T eddy diffusivity
ε dissipation rate per unit mass
ρ bulk density of water–sediment mixture
ν molecular viscosity
ν_T eddy viscosity
ρ_f floc density
ρ_s density of the sediment
ρ_w density of the water due to salinity only
ν_T eddy viscosity
σ_T turbulent Prandtl-Schmidt number
τ_b bed shear stress
ϕ volume concentration
ϕ_* min {1, ϕ}

References

Allen GP, Salmon JC, Bassoullet P, Du Penhoat Y, De Grandpre C (1980) Effects of tides on mixing and suspended sediment transport in macrotidal estuaries. Sed Geol 26:69–90

Cleveringa J (2008) Evolution of sediment volume Ems-Dollard and eastern Dutch Wadden Sea—summary of knowledge and data. Alkyon, report A2274, Emmeloord, The Netherlands (in Dutch)

De Deckere EMGT, Kornman BA, Staats N, Termaat GR, De Winder B, Stal LJ, Heip CHR (2002) The seasonal dynamics of benthic (micro)organisms and extracellular carbohydrates in an intertidal mudflat and their effect on the concentration of suspended sediment. In: Winterwerp JC, Kranenburg C (eds) Fine sediment dynamics in the marine environment, Proceedings in Marine Science, vol 5. Elsevier, Amsterdam, pp 429–440

De Jonge VN (2007) Biological processes in the Ems estuary. Presentation at the LOICZ workshop on the Ems River, February, 2007, Emden, Germany (paper in preparation)

Dickhudt PJ, Friedrichs CT, Schaffner LC, Sanford LP (2009) Spatial and temporal variation in cohesive sediment erodibility in the York River estuary: a biologically-influenced equilibrium modified by seasonal deposition. Mar Geol 267:128–140

Dronkers J (2005) Dynamics of coastal systems. World Scientific, Advanced Series on Ocean Engineering – Volume 25

Dyer KR (1997) Estuaries: a physical introduction. Wiley, Chichester

Friedrichs CT, Armbrust BA, de Swart HE (1998) Hydrodynamics and equilibrium sediment dynamics of shallow, funnel-shaped tidal estuaries. In: Dronkers J, Scheffers M (eds) Physics of estuaries and coastal seas. Balkema, Rotterdam, pp 315–328

Jay DA, Musiak JD (1996) Internal tide asymmetry in channels: origins and consequences. In: Pattiaratchi C (ed) Mixing processes in estuaries and coastal seas. American and Geophysical Union Coastal and Estuarine Sciences Monograph, pp 219-258

Le Hir P (1997) Fluid and sediment 'integrated' modeling application to fluid mud flows in estuaries. Cohesive Sediments. 4th Nearshore and Estuarine Cohesive Sediment Transport Conference INTERCOH '94

Loose M (2008) Morphodynamics Suriname River: study of mud transport and impact due to lowering the fairway channel. Delft University of Technology, Civil Engineering and Geosciences, MSc-thesis 2008-09-04

Nichols M, Poor G (1967) Sediment transport in a coastal plain estuary. ASCE J Waterways Harbors WW4(93):83–95

Postma H (1961) Sediment transport and sedimentation of suspended matter in the Dutch Wadden Sea. Neth J Sea Res 1:148–190

Pritchard DW (1952) Salinity distribution and circulation in the Chesapeake Bay Estuarine System. J Mar Res 11:106–123

Schrottke K, Bartholomä A (2008) Detaillierte Einblicke in die ästuarine Schwebstoffdynamik mittels hochauflösender Hydroakustik. Tagungsband zum Seminar Ultraschall in der Hydrometrie: neue Technik; neuer Nutzen; FgHW/DWA, Koblenz, June 2008, 75-82

Scully ME, Friedrichs CT (2003) The influence of asymmetries in overlying stratification on near-bed turbulence and sediment suspension in a partially mixed estuary. Ocean Dyn 53:208–219

Scully ME, Friedrichs CT (2007) Sediment pumping by tidal asymmetry in a partially-mixed estuary. J Geophys Res 112: C07028. doi:10.1029/2006JC003784

Stelling GS (1995) Compact differencing for stratified surface flow. In: Advances in Hydro-Science and –Engineering, II (A) 378-386, Tsinghua University Press, Beijing, China

Talke SA, De Swart HE, Schuttelaars HM (2009) Feedback between residual circulation and sediment distribution in highly turbid estuaries: an analytical model. Continental Shelf Research. doi:10.1016/j.csr.2007.09.002

Van Leussen W (1994) Estuarine macroflocs – their role in fine-grained sediment transport. PhD-thesis, Utrecht University, The Netherlands

Van Leussen W (2009) Macroflocs, fine-grained sediment transports and their longitudinal variations in the Ems estuary. Ocean Dynamics, in press

Van Rijn LC (1993) Principles of sediment transport in rivers, estuaries and coastal seas. AQUA, The Netherlands

Winterwerp JC (1998) A simple model for turbulence induced flocculation of cohesive sediment. IAHR, J Hydraul Eng 36 (3):309–326

Winterwerp JC (2001) Stratification of mud suspensions by buoyancy and flocculation effects. J Geophys Res 106(10):22,559–22,574

Winterwerp JC (2002) On the flocculation and settling velocity of estuarine mud. Cont Shelf Res 22:1339–1360

Winterwerp JC (2006) Stratification effects by fine suspended sediment at low, medium and very high concentrations. Geophysical Research 111(C05012):1–11

Winterwerp JC, Van Kesteren WGM (2004) Introduction to the physics of cohesive sediment in the marine environment. Elsevier, Developments in Sedimentology, 56

Winterwerp JC, Wang ZB, Van der Kaaij T, Verelst K, Bijlsma A, Meersschaut Y, Sas M (2006) Flow velocity profiles in the Lower Scheldt estuary. Ocean Dyn 56:284–294